JOURNAL OF VIROLOGY, July 1996, p. 4632–4645 Vol. 70, No. 7
0022-538X/96/$04.00+0

Direct Interactions of Coxsackievirus B3 with Immune Cells in the Splenic Compartment of Mice Susceptible or Resistant to Myocarditis

DANIEL R. ANDERSON,[1,2] JANET E. WILSON,[1] CHRISTOPHER M. CARTHY,[1] DECHENG YANG,[1] REINHARD KANDOLF,[3,4] AND BRUCE M. MCMANUS[1]*

Department of Pathology and Laboratory Medicine, University of British Columbia—St. Paul's Hospital, Vancouver, Canada[1]; Department of Pathology and Microbiology, University of Nebraska Medical Center, Omaha, Nebraska[2]; and Institute of Pathology, Department of Molecular Pathology, University of Tübingen, Tübingen,[3] and Max Planck Institute for Biochemistry, Department of Virus Research, Martinsried,[4] Germany

Received 30 November 1995/Accepted 5 April 1996

In vitro replication of coxsackievirus B3 (CVB3) in cells of the immune system derived from uninfected adolescent A/J and C57BL/6J mice and replication of CVB3 in and association with immune cells from spleens of infected animals in vivo were assessed. Nonstimulated or mitogen-stimulated spleen cells were minimally permissive for viral replication during an 8-h period. Three days postinfection (p.i.), CVB3 RNA was localized in vivo to B cells and follicular dendritic cells of germinal centers in both A/J and C57BL/6J mice; however, extrafollicular localization was greater in C57BL/6J mice ($P = 0.0054$). Although the pattern of CVB3 RNA localization was different, the total load of infectious virus (PFU per milligram of tissue) was not different. Splenic CVB3 titers (PFU per milligram of tissue) in both strains were maximal at day 3 or 4 p.i. and were back to baseline by day 7 p.i., with most infectious virus being non-cell associated. CVB3 titers (PFU per milligram of tissue) correlated directly with in situ hybridization positivity in splenic follicles and extrafollicular regions in both murine strains; however, follicular hybridization intensity was greater in A/J mice at day 5 p.i. ($P = 0.021$). Flow cytometric analysis demonstrated that 50.4% of total spleen cells positive for CVB3 antigen were B cells and 69.6% of positive splenic lymphocytes were B cells. Myocardial virus load in C57BL/6J mice was significantly lower than that in A/J mice at days 4 and 5 p.i. These data indicate that CVB3 replicates in murine splenocytes in vitro and in B cells and extrafollicular cells in vivo.

Enteroviruses, including coxsackieviruses, have been studied in humans as well as in murine models for the past 4 decades; however, the exact role of enterovirus infections in the pathogenesis of human diseases, including myocarditis and idiopathic dilated cardiomyopathy, is still debated (41, 42). Primary focuses of studies with regard to coxsackievirus B3 (CVB3) have been the extent of myocardial replication and cell damage, the evolutionary phenomenon of early and late virus-induced myocarditis, the potential relationship of enteroviral persistence to heart failure (12, 42, 43), and the role of inflammatory responses in the development of CVB3-induced diseases (17, 25, 64, 65). Few studies thus far have evaluated the role of CVB3 infections of the immune system itself or the consequences of such infections (7, 37, 38, 40).

Over the past 3 decades, intriguing associations between many different viruses and virtually every element of the immune system have been observed (39, 47, 49, 62). The pathogenetic significance of these associations has only recently been examined (1, 2, 16, 50, 56), and these phenomena are increasingly perceived as key events in viral pathogenesis. A paradigm is emerging, related to virus-immune cell interactions as a critical balance between host and/or viral adaptation.

The ability of the host's immune system to respond appropriately to a virus infection during the early and late stages of disease is the matter in question. We have established previously by in situ hybridization (ISH) the differential localization of viral RNA in spleens of adolescent, myocarditis-susceptible A/J ($H\text{-}2^a$), and myocarditis-resistant C57BL/6J ($H\text{-}2^b$) mice infected with CVB3 (12). We now present data which clearly document CVB3 association with and replication in (i) murine splenic immune cells in vitro and (ii) B cells and extrafollicular cells in vivo. These interactions may underpin the severity of target organ injury and the pattern of virus-induced disease in different strains of mice.

* Corresponding author. Mailing address: Cardiovascular Research Laboratory, McDonald Research Wing, St. Paul's Hospital, 1081 Burrard St., Vancouver, B.C., Canada V6Z 1Y6. Phone: (604) 631-5200. Fax: (604) 631-5208. Electronic mail address: mcmanus@unixg.ubc.ca.

MATERIALS AND METHODS

Experimental designs. Unsorted splenocytes from uninfected A/J and C57BL/6J mice (Jackson Laboratories, Bar Harbor, Maine) were isolated, infected with CVB3, and cultured for 2, 4, 6, 8, 12, 24, and 48 h. Splenocytes that were nonstimulated, stimulated (with concanavalin A [ConA] or lipopolysaccharide [LPS]) at 24 h before infection ($t = -24$), or stimulated (with ConA or LPS) at the time of infection ($t = 0$) were evaluated for infectious CVB3 particles and RNA. Mean infectious CVB3 yields after in vitro culture were determined by three individual experiments utilizing cells isolated from different animals.

A series of separate experiments have been performed and are presented in this work. A/J ($n = 3$ per group) and C57BL/6J ($n = 3$ per group) mice were infected intraperitoneally with 10^5 PFU of CVB3. At days 1, 2, 3, 4, and 7 postinfection (p.i.), mice were killed and the heart, liver, spleen, and pancreas of each mouse were harvested and triaged (experiment 1). As well, A/J ($n = 10$ per group) and C57BL/6J ($n = 10$ per group) mice were evaluated at days 3, 4, 5, and 6 p.i. (experiment 2). After these initial two experiments, animals ($n = 5$ per group) were evaluated at day 3 p.i. Explant splenic sections were cultured for 18 h in RPMI at 37°C and immediately postculture were fixed in 4% paraformaldehyde prior to being embedded in paraffin. A portion of selected spleens was utilized for the isolation of immune cells. The direct viral damage of these organs was evaluated by light microscopy, and the concentration of virus was evaluated by plaque assay (9, 12, 45). Viral RNA was evaluated by ISH and reverse transcription-PCR (RT-PCR) (11, 23), with modifications (44). Viral and immune cell antigens were evaluated by immunohistochemistry (IHC) and flow cytometry (33).

Virus and animals. Stock CVB3 was generously provided by Charles J. Gauntt and was stored at −80°C. Virus was grown in HeLa cells (American Type

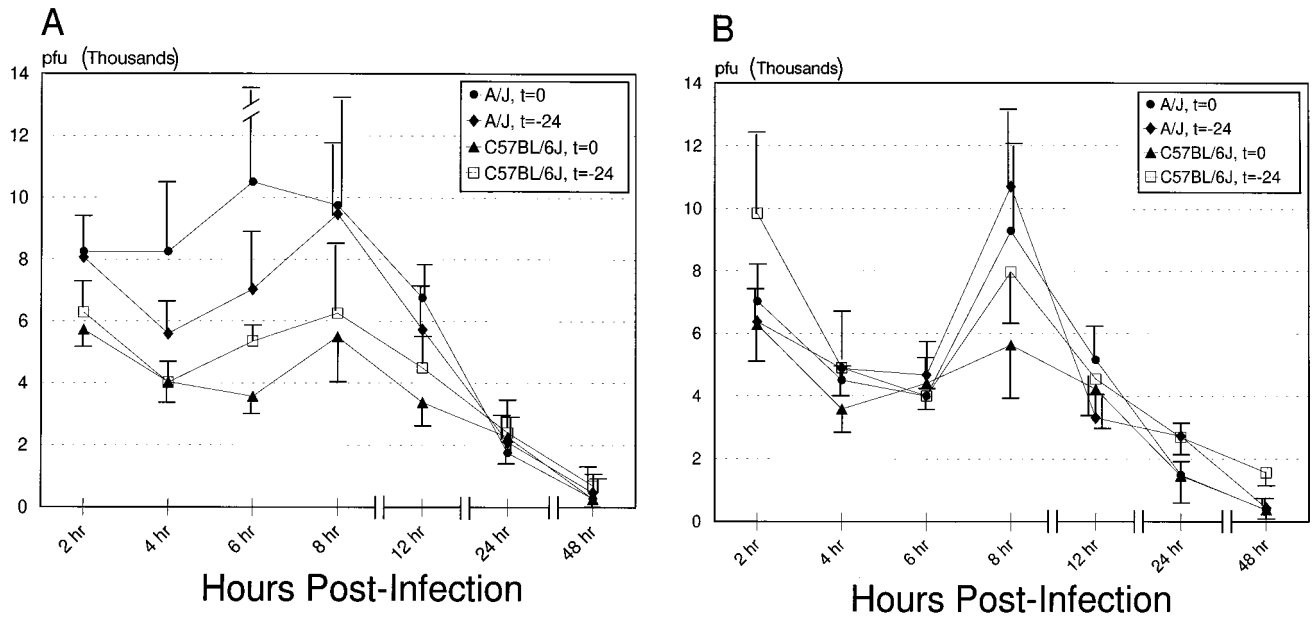

FIG. 1. This figure shows the titers of infectious virus in splenocytes isolated from uninfected A/J and C57BL/6J mice after in vitro CVB3 infection. Each datum point reflects the mean of three separate experiments utilizing splenocytes isolated from one mouse per experiment. Each line reflects the change in virus concentration over time in tissue culture supernatant of mixed splenocytes under the following conditions: not stimulated with a mitogen (broken error bar = 5,484 PFU) (A), stimulated with ConA (B), and stimulated with LPS (C), either 24 h prior to infection ($t = -24$) or at the time of infection ($t = 0$). Error bars, standard errors.

Culture Collection, Rockville, Md.), and titers were routinely redetermined at the beginning of all individual experiments.

Animals were 4 weeks of age when received at St. Paul's Hospital animal care facility, University of British Columbia, and 5 weeks of age at the onset of each experiment. Mice were sacrificed by CO_2 narcosis, and the appropriate tissues and blood were triaged and utilized according to the following protocols. Animals that died naturally after virus infection were autopsied and evaluated as such. Only tissues obtained from animals killed at the defined experimental time points were included in the mean data of an experimental group.

Preparation of single-cell suspensions of immune cells (13). Single-cell suspensions of splenocytes were prepared by delicate homogenization of the spleen in a Wheaton glass tissue homogenizer. Tissue debris was discarded, the cell suspension was centrifuged ($500 \times g$, 5 min), and the supernatants were archived for plaque assay. Erythrocytes were eliminated from the cell pellet by shock lysis with 0.1 M Tris (pH = 7.2) and 0.16 M NH_4Cl (5 min, 4°C), centrifuged, and resuspended. Cell counts were determined on a hemocytometer and/or on a Coulter counter (model S880).

Preparation of immune cells for in vitro culture and activation of lymphocytes. Single-cell suspensions of lymphocytes (see above) from separate animals from each mouse strain were made in complete RPMI-1640 (penicillin-streptomycin [10,000 U/ml], L-glutamine [200 mM], HEPES [*N*-2-hydroxyethylpiperazine-*N*′-2-ethanesulfonic acid] buffer [10 mM], and 10% fetal bovine serum [non-heat inactivated]; Sigma Chemical Co., St. Louis, Mo.) with 2-mercaptoethanol (0.05 mM). Non-heat-inactivated serum was used in these particular cultures with the view that complement components may facilitate virus-cell interactions (8, 54). Cells were infected with CVB3 at a multiplicity of infection of 5 (1 h, 37°C, 5% CO_2) and washed three times in Dulbecco's phosphate-buffered saline (DPBS) (Gibco/BRL, Grand Island, N.Y.). For activation of lymphocytes, single-cell suspensions (10^7 cells per ml of complete RPMI-1640) were incubated (37°C, 5% CO_2) with either 2.5 μg of ConA (Sigma Chemical Co.) per ml or 25 μg of LPS (Sigma Chemical Co.) per ml per experimental design. Optimal mitogenic concentrations of ConA and LPS were determined by a ^3H proliferation assay (14).

Flow cytometry. Single-cell suspensions of lymphocytes from CVB3-infected or uninfected animals were adjusted to 2×10^7 cells per ml in DPBS and stained with an anti-CD45R antibody, a B-cell surface marker (B220 isoform, clone RA3-6B2) diluted 1:200 in DPBS, which is directly conjugated to fluorescein isothiocyanate (Gibco/BRL). Cells were washed three times with DPBS and then fixed with 10% buffered formalin (overnight, 4°C). After being washed three times with TSK-BT (100 mM Tris-base, 550 mM NaCl, 10 mM KCl, 2% bovine serum albumin, 0.1% Triton X-100 [to permeablize]), immune cells were blocked with normal goat serum and anti-Fc receptor antibody (PharMingen, San Diego, Calif.), both at 1:250 dilution in TSK-BT (5 min, room temperature [r.t.]). Cells were then stained for the presence of viral antigens with a rabbit anti-CVB3 polyclonal antibody (Accurate Chemical and Scientific Co., Westbury, N.Y.) at a 1:250 dilution in TSK-BT (30 min, r.t.), washed three times (TSK-BT), stained with an $F(ab')_2$ donkey anti-rabbit (heavy- and light-chain) antibody conjugated to R-phycoerythrin (Jackson ImmunoResearch Laboratories, Inc., Westgrove, Pa.) (30 min, r.t.), washed three times (TSK-BT), and fixed again in 10% buffered formalin. Cells were then analyzed on a Coulter flow cytometer. Experimental results for each sample reflect percentages determined from more than 1,000 fluorescent events.

Tissue histopathology (12). Transverse ventricular sections from the heart as well as those from the spleen, liver, and pancreas were fixed in Bouin's solution (2 h, r.t.) or fresh DPBS-buffered 4% paraformaldehyde (12 h, 4°C) and embedded in paraffin. Paraffin blocks were sectioned for IHC and ISH. Sections were also stained with hematoxylin and eosin or Masson's trichrome stain. The extent and severity of virus-induced disease in the spleen, heart, liver, and pancreas were blindedly evaluated on a scale of 0 to 5+/5+ (least to most) for overall disease, including coagulation necrosis, contraction band necrosis, and cytopathic effects as previously described (12).

FIG. 2. ISH shows positive staining for the sense-strand (A and D) and antisense-strand (B and E) RNA of CVB3 in A/J (A and B) and C57BL/6J (D and E) nonstimulated mixed splenocytes infected in vitro and harvested 6 h p.i. Arrowheads indicate splenocytes with definitive positive signals. For comparison, uninfected negative control splenocytes from A/J and C57BL/6J mice are shown (C and F, respectively). (F) Bar = 10 μm.

Virus content of tissue. The titers of CVB3 in tissues, cell supernatants, or sera were determined on monolayers of HeLa cells (American Type Culture Collection) by agar overlay plaque assay in duplicate, with modifications (9, 12, 45). HeLa cells are routinely tested for *Mycoplasma* infections (21). Fresh frozen tissues or cells were homogenized with an OMNI 2000 homogenizer equipped with a 5-mm-diameter generator. Multiple samples were serially diluted 10-fold and overlaid on 95 to 100% confluent monolayers of HeLa cells in 6-well plates and were incubated (5% CO_2, 1 h, 37°C). Virus was removed by pipetting, and warm medium (minimal essential medium plus penicillin-streptomycin [10,000 U/ml], L-glutamine [200 mM], HEPES buffer [238.3 g/liter], 10% fetal bovine serum [heat inactivated], and 0.75% agar) was overlaid in each well. The plates were incubated (2 to 3 days, 5% CO_2, 37°C), fixed with Carnoy's fixative (30 min), and stained with 1% crystal violet. The plaques were counted, and the viral concentration was calculated as PFU per milligram of wet tissue, number of cells, or milliliter.

IHC. Rat anti-mouse CD45R (B220 isotype, clone RA3-6B2) (Gibco/BRL) was used at a dilution of 1:100. Small pieces of tissues (approximately 3 mm^3) were fixed in Bouin's solution (2 h, r.t.) or fresh DPBS-buffered 4% paraformaldehyde (12 h, 4°C), dehydrated in graded alcohols, and embedded in warm paraffin (temperature, <60°C). IHC was performed as described previously (33) with modifications as detailed below.

Tissue sections (2 μm thick) were placed onto Superfrost glass slides (VWR Scientific, Toronto, Canada), baked (2 h, 60°C), dewaxed in xylenes, and dipped in 100% alcohol. The slides were then incubated in 3% H_2O_2–97% methanol (30 min, r.t.), rehydrated in graded alcohols, rinsed in tap water, and incubated in 20 mM citrate buffer (pH = 3.2; 15 min, r.t.).

One hundred microliters of blocking solution (TSK-BT, 1% normal serum of the species of the primary antibody, and avidin D blocker [Vector Laboratories, Burlingame, Calif.]) was applied to each slide, incubated (1 h, r.t.), and rinsed once with DPBS. One hundred microliters of optimally diluted primary antibody (diluted in TSK-BT, 1% normal serum, 0.5% normal mouse serum, and biotin blocker [Vector Laboratories]) was applied to each slide, incubated (overnight, r.t.), and rinsed three times with DPBS. Negative control sections were stained with normal serum at the same dilution in place of the primary antibody. The secondary biotinylated immunoglobulin (diluted 1:200 in TSK-BT–0.5% normal mouse serum; Vector Laboratories) was applied, and this was followed by the application of avidin-biotin-horseradish peroxidase complex (Vector Laboratories). DAB (3,3′-diaminobenzidine tetrahydrochloride with nickel ions and hydrogen peroxide) (Pierce ImmunoTechnology, Rockford, Ill.) substrate was added and allowed to develop. Slides were lightly counterstained with hematoxylin, dehydrated in graded alcohols, dipped in xylenes, and covered with coverslips.

Enterovirus-specific ISH. Enterovirus-specific ISH was performed on both cell cytospin preparations from in vitro infections and tissue sections as described previously (11, 23), with modifications as described elsewhere (44). Briefly, tissue was fixed in 4% paraformaldehyde or Bouin's solution, embedded in paraffin, sectioned, placed onto silanated or Superfrost glass slides, baked, dewaxed, and rehydrated in graded alcohols. Both the tissue and cells were then permeabilized, dehydrated in graded alcohols, dried, and hybridized. The hybridization mixture contained a digoxigenin-labelled viral strand-specific riboprobe (sense or antisense strand) (nucleotide [nt] 1 to 7127 and 888 to 7127, respectively) transcribed from the infectious cDNA as previously described (23). From 21 to 29 μl of hybridization mixture was applied. The slides were heated (75°C, 10 min), and hybridization was allowed to proceed in a humidified chamber. Posthybridization washing was followed by blocking with 2% normal lamb serum. A sheep anti-digoxigenin polyclonal antibody, conjugated to alkaline phosphatase (Boehringer Mannheim, Laval, Canada), was enzymatically developed for 48 to 96 h (Sigma-Fast nitroblue tetrazolium-BCIP [5-bromo-4-chloro-3-indolylphosphate toluidinium; Sigma Chemical Co.). Hybridization positivity in the pancreas and heart is apparent within minutes to 2 h of substrate application; however, positivity in the spleen is typically only detectable after 24 to 48 h of development. The slides were subsequently counterstained with eosin or carmalum and examined quantitatively for reaction product by light microscopy. The distribution and intensity of ISH positivity were evaluated and scored blindedly on a scale of 0 to 5+/5+ (least to most) for the tissue being evaluated. For the heart, a score of 0+ reflects 0% cell positivity for CVB3 RNA, 1+ reflects <10% positivity, 2+ reflects 10 to 20% positivity, 3+ reflects 30 to 40% positivity, 4+ reflects 40 to 50% positivity, and 5+ reflects >50% positivity. For splenic follicles, a score of 0+ reflects 0% splenic follicles positive for CVB3 RNA, 1+ reflects 10 to 20% positivity, 2+ reflects 20 to 40% positivity, 3+ reflects 40 to 60% positivity, 4+ reflects 60 to 80% positivity, and 5+ reflects >80% positivity. Extrafollicular regions of the spleen, liver, and pancreas were scored similarly where relevant.

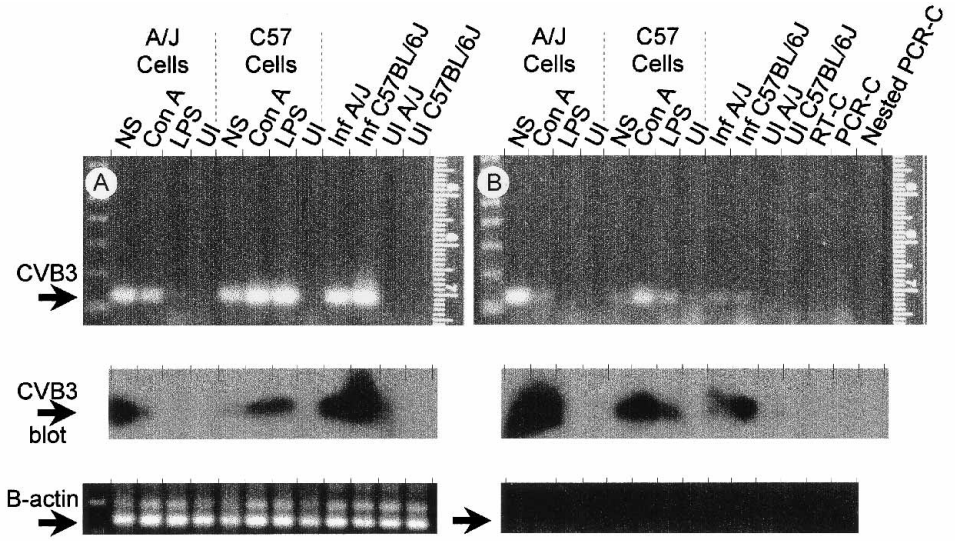

FIG. 3. Nested RT-PCR products (135 bp) of the sense-strand (A) or antisense-strand (B) RNA of CVB3 are detectable in RNA isolated from A/J and C57BL/6J mixed splenocytes (cells) not stimulated with a mitogen (NS) or stimulated with ConA or with LPS. Uninfected, nonstimulated (UI) A/J and C57BL/6J mixed splenocytes are negative for CVB3 nested RT-PCR products. In vivo-infected A/J (Inf A/J) and C57BL/6J (Inf C57BL/6J) mice are positive for nested RT-PCR products from the sense-strand RNA (A) or antisense-strand RNA (B), while uninfected A/J (UI A/J) and C57BL/6J (UI C57BL/6J) mice are negative. RT, PCR, and nested PCR H_2O negative controls are negative (RT-C, PCR-C, and Nested PCR-C, respectively). Southern blotting of the DNA products with a digoxigenin probe confirmed the presence of the respective CVB3 sense and antisense viral RNA sequences. All RNA isolates are positive for RT-PCR products of β-actin (245 bp) with the 3′ primer (sense) but are negative for β-actin products with the 5′ primer (antisense). The latter confirms that the PCR-amplified DNA (i.e., specific sense or antisense sequences) reflects RT products generated from viral RNA or β-actin by SuperScript RNase H^- reverse transcriptase and not *Taq* DNA polymerase (46, 59).

RT-PCR, nested PCR, and blotting. RT-PCR was optimized for $MgCl_2$ concentration, annealing temperature, and cycle number in the RT and PCR steps for each primer or primer set (27). The sensitivity of nested PCR has been established in our laboratory, and this procedure affords the detection of 1.5 to 15 copies of viral RNA in 5 ng of nonspecific RNA by ethidium bromide staining (4a, 52).

The following primers were synthesized (Oligonucleotide Synthesis Laboratory, University of British Columbia) and used in the RT-PCR steps. Primers E_1 and E_2 (nt 625 to 642 and 448 to 462, respectively) have previously been described by Chapman et al. (10), and primer D (nt 581 to 601) was described by Jin et al. (28). Primer C_2 (nt 467 to 486) and probe EF (nt 537 to 565) were designed from the CVB3 sequence by Klump et al. (32). Primers E_1 and E_2 yield a 195-bp fragment, and primers D and C_2 yield a 135-bp fragment. Murine β-actin primers (Stratagene, La Jolla, Calif.) were used for positive RNA controls. Negative controls, in which water was substituted for the RNA sample, were included in every run.

In brief, optimized RT (3 mM $MgCl_2$) was carried out in a 10-μl reaction volume with SuperScript RNase H^- reverse transcriptase (Gibco/BRL), 50 pM E_1 or E_2, and 5 ng of RNA. High-quality RNA ($A_{260}/A_{280} \geq 1.7$) was isolated utilizing RNA spin columns (Rneasy; Qiagen Inc., Chatsworth, Calif.). The RT reaction mixture was cycled once (42°C for 50 min, 95°C for 5 min, 4°C soak) in a Perkin-Elmer Cetus DNA 9600 thermal cycler. For the detection of strand-specific priming by the 3′ or 5′ primer, RNase A (10 ng) was added to each reaction tube and incubated (15 min, 37°C) prior to PCR to ensure that cDNA synthesis was not due to RT of viral RNA by *Taq* DNA polymerase during the 35 cycles of PCR and 30 cycles of nested PCR at standard $MgCl_2$ concentrations (46, 59).

To the resulting cDNA RT mixture, 40 μl of the PCR solution (3.25 mM $MgCl_2$, *Taq* DNA polymerase, 50 pM primers E_1 and E_2, and 0.44 μg of Taq-Start antibody [ClonTech Laboratories Inc., Palo Alto, Calif.]) was added. The PCR mixture was denatured (95°C for 5 min) and cycled 35 times (52°C for 30 s, 72°C for 10 s, and 95°C for 30 s).

For nested PCR, 5 μl of the PCR mixture was added to 45 μl of the nested-PCR cocktail (*Taq* DNA polymerase, 3.5 mM $MgCl_2$) and 50 pM primers D and C_2. The PCR mixture was denatured (95°C for 5 min) and cycled 30 times (60°C for 30 s, 72°C for 10 s, and 95°C for 30 s).

The PCR products were electrophoresed at 100 to 150 V into 2% agarose gels with ethidium bromide in 0.5× TAE (20 mM Tris acetate [pH = 7.8] and 0.5 mM EDTA) and evaluated. Southern blotting assays were performed as follows. DNA bands were transferred from the agarose gel to Nytran (Schleicher &

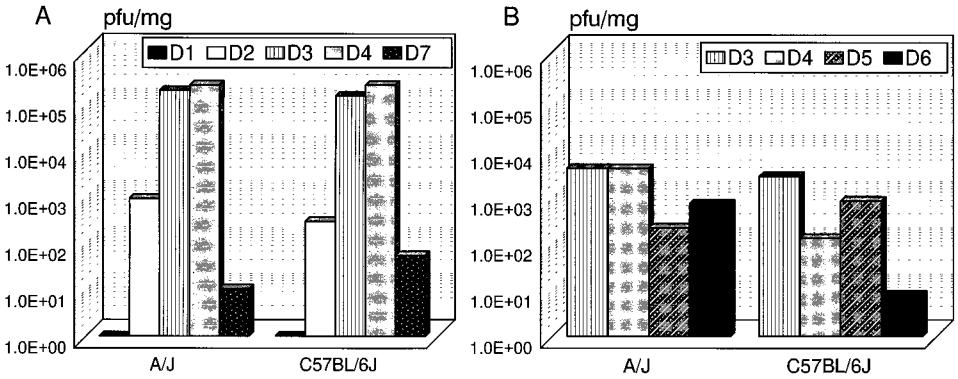

FIG. 4. The concentrations of CVB3 (PFU per milligram) in the spleens of A/J and C57BL/6J mice as determined by plaque assay from day 1 through 7 p.i. (D1 to D7) in two separate experiments are shown. Each bar represents the mean value for 3 or 10 animals (experiments 1 and 2 [A and B], respectively). There is no significant difference in the concentration of CVB3 in the spleens for A/J or C57BL/6J mice at any time point p.i. 1.0E+04 = 10^4.

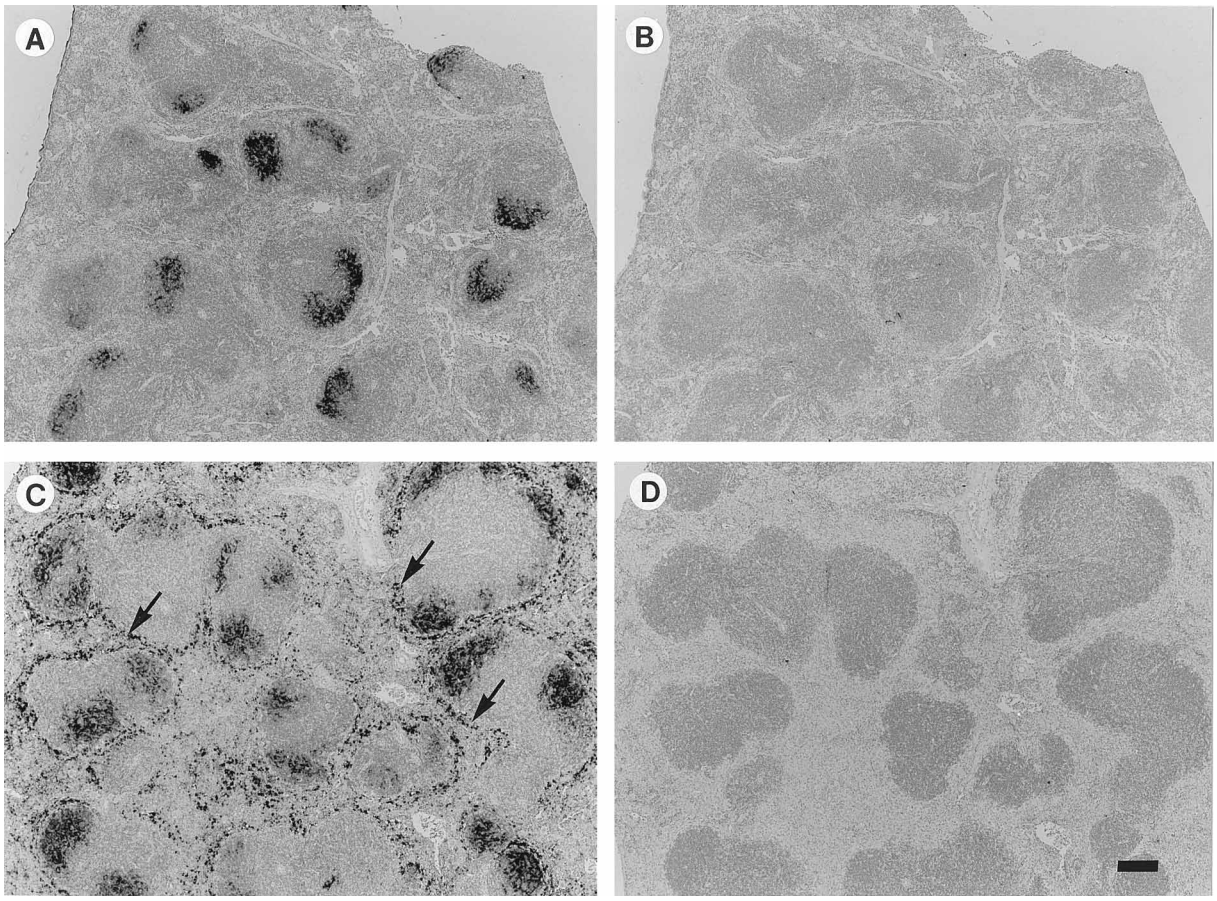

FIG. 5. ISH positivities for the sense-strand (A and C) and antisense-strand (B and D) viral RNA in the spleens of A/J (A and B) and C57BL/6J (C and D) mice at day 3 p.i. are shown. Note the difference in the staining pattern of the A/J strain versus the C57BL/6J strain, specifically the extrafollicular ISH positivity (arrows) for CVB3 RNA in C57BL/6J mice. (D) Bar = 200 μm.

Schuell Inc., Keene, N.H.) with an Owl semidry blotter and were baked. Hybridization of transferred DNA was performed with an oligonucleotide (probe EF) tailed with digoxigenin-labelled dUTP by using terminal transferase (Boehringer Mannheim). The Nytran membranes were prehybridized, probed, washed, blocked, and stained with a sheep antidigoxigenin antibody conjugated to alkaline phosphatase (Boehringer Mannheim) diluted 1:20,000. The membranes were washed and dipped in CDP-*Star* (Boehringer Mannheim) chemiluminescent substrate (1 min, r.t.). X-ray films were exposed for 3 min and developed.

Statistical analysis. When comparisons between groups were made, data were analyzed by Student's *t* test by utilizing Systat software (57). Bonferroni probabilities were applied when multiple *t* test comparisons were made within a particular experiment (24). Pearson product-moment correlation was used in relating infectious virus to genomic positivity by hybridization (57). Results were considered statistically significant when the probability of a type I error was less than 0.05.

RESULTS

In vitro replication of CVB3 in splenocytes. To determine whether CVB3 replicates in immune cells, the in vitro infection of mixed splenocytes was evaluated. Cells were cultured in complete RPMI-1640 or stimulated with ConA or LPS and evaluated for capacity for replication of infectious virus by a plaque assay method and evaluated for viral RNA synthesis by ISH and nested-RT-PCR methods. The replication of virus was minimal in these cells, and nascent infectious virus was barely detectable by the plaque assay method. Incubation of cells with ConA did not quantitatively affect the production of infectious virus in isolated naive splenic immune cells compared with that in nonstimulated cells over the time course of

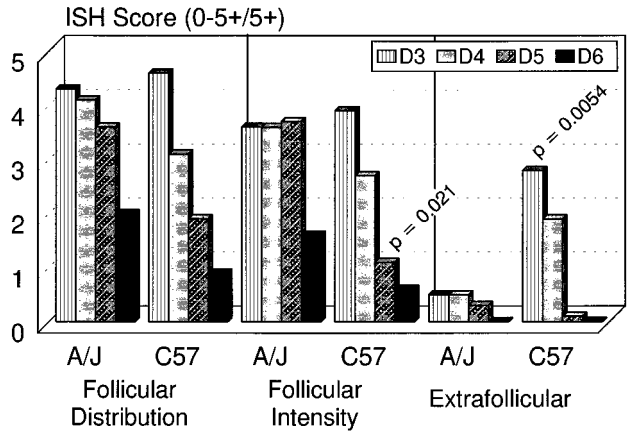

FIG. 6. These bar graphs represent the mean ISH distribution and intensity scores of A/J and C57BL/6J splenic follicular and extrafollicular regions on days 3 to 6 p.i. (D3 to D6) (n = 7 to 10 per group). Each bar represents a score derived from one ISH section from each of the animals per group per day p.i. The distribution of viral RNA positivity in A/J follicles was not significantly different than that for C57BL/6J mice at any day p.i.; however, the intensity of viral RNA staining in A/J follicles was significantly greater than that for C57BL/6J mice at day 5 p.i. (P = 0.021). With regard to ISH staining in the extrafollicular regions of the spleen (marginal zone and red pulp), A/J extrafollicular staining was significantly less than that for C57BL/6J mice at day 3 p.i. (P = 0.0054).

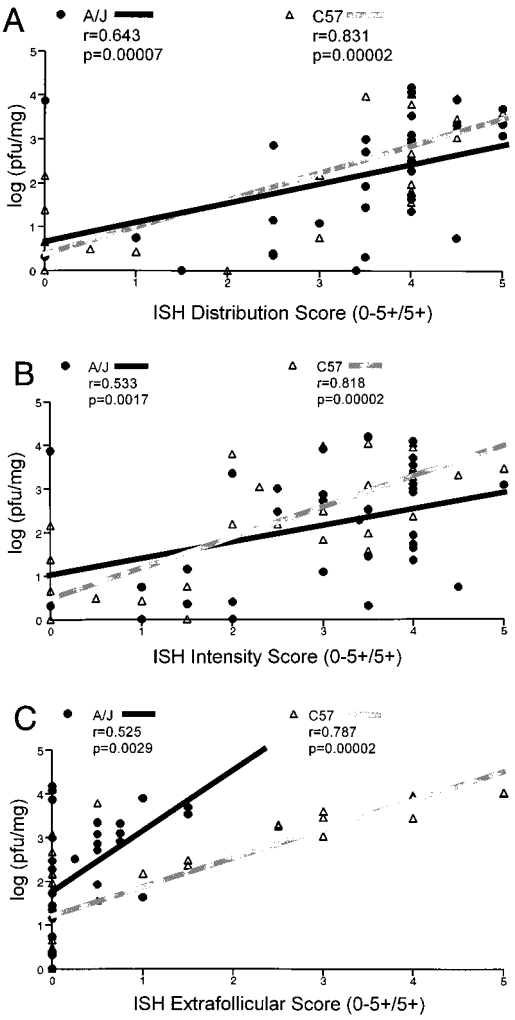

FIG. 7. Correlation of ISH follicular distribution (A), follicular intensity (B), and extrafollicular scores (C) with infectious CVB3 (PFU per milligram) in spleens of A/J ($n = 34$) and C57BL/6J mice ($n = 34$). Plaque assay and ISH datum points represent all animals on days 3 to 6 p.i. The Pearson product-moment correlations with infectious CVB3 are shown at the top of each panel.

evaluation (Fig. 1A and B); however, when cells were incubated with LPS, the production of infectious virus was abolished (Fig. 1C). There was a characteristic pattern of viral titers in these cells after challenge (Fig. 1A and B). For both mouse strains, virus concentration in the cell supernatant decreased between 2 and 6 h p.i. with a subsequent small increase to peak levels at 8 h p.i. These levels then decreased gradually over the next 40 h p.i. From 8 to 48 h, the decrease in virus titer reflects the inactivation of virus due to incubation at 37°C, as determined by incubation of virus stock alone (data not shown). At 8 h p.i., the stimulated and nonstimulated splenocyte cultures from the myocarditis-susceptible strain (A/J) produced more infectious virus than did splenocytes from the myocarditis-resistant strain (C57BL/6J) at both time points of virus challenge ($t = -24$ h and $t = 0$ h) (Fig. 1A and B). ISH was performed on the same cells (Fig. 2A to D) to detect the presence of sense- and antisense-strand RNA and confirm our plaque assay data indicating that virus replicates in splenocytes which are nonstimulated. As well, ISH revealed the presence of antisense-strand CVB3 RNA in ConA- and LPS-stimulated splenocytes (data not shown). Furthermore, the presence of sense- and antisense-strand RNA was evaluated by RT-PCR and nesting of PCR products. RNA isolated from nonstimulated or mitogen-stimulated ($t = -24$) splenocytes 6 h post-viral challenge contained detectable sense- and antisense-strand viral RNA (Fig. 3). Thus, sense- and antisense-strand RNA were detected in all RNA isolates after RT-PCR and nesting and/or Southern blotting (Fig. 3). The presence of the antisense-strand RNA confirms virus replication in a portion of these cells.

In vivo distribution of CVB3 RNA in immune compartments. To evaluate the association of CVB3 with splenocytes, the temporal load of infectious virus in the spleens of A/J and C57BL/6J mice during the early stage of disease (days 1 through 7) was determined. The concentration of infectious CVB3 (PFU per milligram) in the spleens of specific animals was detectable but low at days 1 and 2 p.i., and in both strains, the concentration of virus increased dramatically and was maximal by days 3 to 4 p.i. and decreased by days 5 to 7 p.i. (Fig. 4). There was no significant difference between the total loads of infectious virus in the spleens of the two strains of mice. This similarity in virus load was observed when the noncellular fractions of spleens were analyzed on days 3 or 4 in both strains; however, most virus detected resided in the noncellular fraction (10-fold more than in the cellular fraction) (data not shown). The cell association of infectious virus was consistently found to be somewhat greater in the C57BL/6J strain than in the A/J strain (data not shown).

ISH for CVB3 sense-strand RNA in these same tissues corroborated the presence of infectious virus in the spleen as determined by plaque assay. The distribution and intensity of viral RNA hybridization staining within the spleen, however, was distinctive between strains in extrafollicular localization of viral RNA during early infection (Fig. 5 and 6). In A/J mice (the myocarditis-susceptible strain), virus localized to the germinal centers of lymphoid follicles (Fig. 5 and 6). In C57BL/6J mice (myocarditis-resistant strain), virus localized not only to the germinal centers but also to the marginal zone and red pulp (Fig. 5 and 6). Total data from both strains show that there was a concomitant increase in ISH positivity in splenic tissues with increasing infectious viral load (Fig. 7). The distribution of ISH positivity in the follicles at all time points p.i. correlated with the concentration of infectious virus (PFU per milligram) in the spleens of A/J ($r = 0.643$; $P = 0.00007$) and C57BL/6J ($r = 0.831$; $P = 0.00002$) mice (Fig. 7A). The intensity of hybridization in the follicles of both A/J and C57BL/6J mice was also correlated with the concentration of infectious virus in the spleens of A/J ($r = 0.533$; $P = 0.0017$) and C57BL/6J ($r = 0.818$; $P = 0.00002$) mice (Fig. 7B). Finally, hybridization in the extrafollicular region of the spleen was also correlated with the concentration of infectious virus in the spleens of A/J ($r = 0.525$; $P = 0.0029$) and C57BL/6J ($r = 0.787$; $P = 0.00002$) mice (Fig. 7C). These data show that both sense- and antisense-strand RNAs are detected in the spleens of either murine strain and that the amount of sense strand correlated with the amount of infectious virus present.

With regard to CVB3 infection of other immune system compartments, characteristic infection patterns were found in lymph nodes and in liver sinusoidal cells (Kupffer cells; F4/80 antibody positive). In lymph nodes there was ISH positivity for sense-strand RNA in germinal centers, the subcapsular sinus, and in the medullary cords (data not shown). In the liver, virus was found in Kupffer cells and hepatocytes (data not shown).

We have demonstrated CVB3 replication in splenic tissue obtained at autopsy by showing ISH positivity for the sense- and antisense-strand viral RNA in both germinal centers and

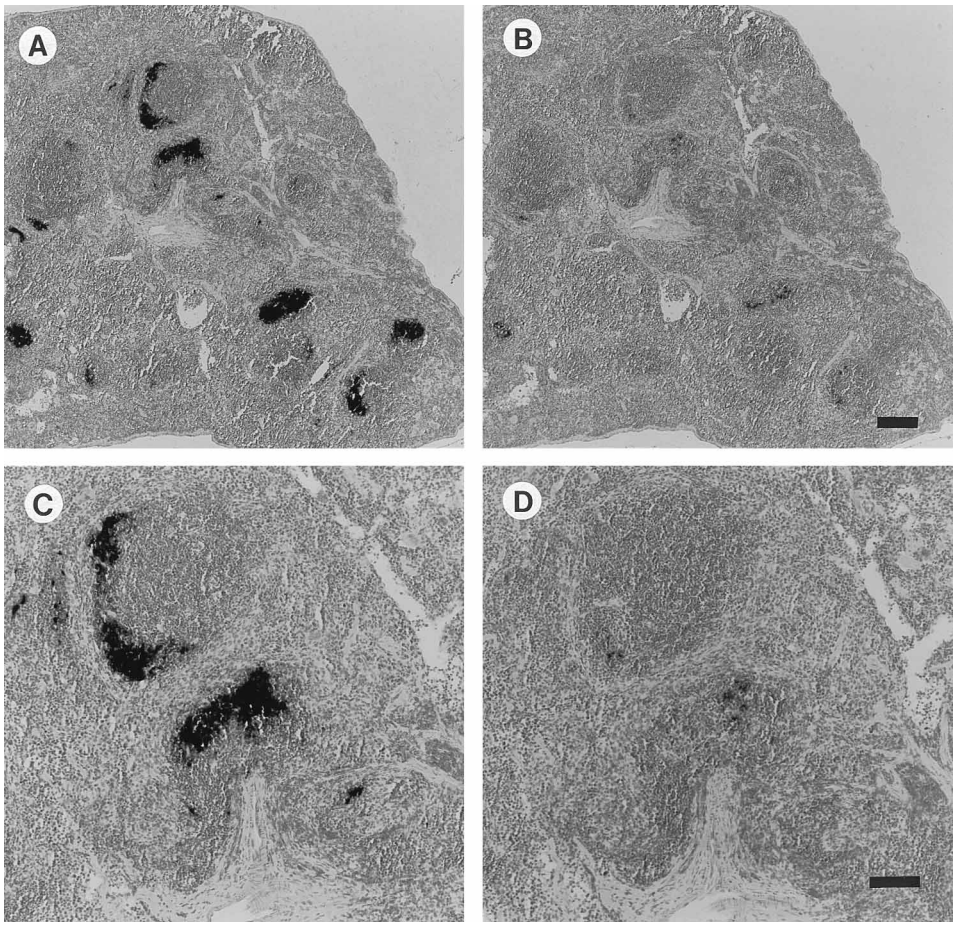

FIG. 8. ISH for sense and antisense RNA in the spleen from an A/J mouse autopsied within 12 h of death. The sense-strand (A and C) and antisense-strand (B and D) RNAs were detectable in contiguous sections in the same germinal centers and cells. (B) Bar = 200 μm (also for panel A); (D) bar = 100 μm (also for panel C).

extrafollicular cells on contiguous tissue sections (Fig. 8). We also evaluated splenic tissues which were fixed after culture for 18 h (Fig. 9A to F). For both strains of mice (C57BL/6J data not shown), the intensity of ISH staining in the same spleen for sense-strand RNA was increased after culture (Fig. 9A, C, and E) and contiguous sections of cultured tissue were positive for the antisense-strand RNA in germinal centers and extrafollicular cells (Fig. 9D and F). There were, however, few cells in C57BL/6J spleens which were positive for antisense-strand RNA. It is of particular interest that the intensity of staining, and thus the ratio of sense- to antisense-strand RNA, in cultured spleens was different than that in the heart (23, 31). When antisense-strand RNA is detectable in the same cell of contiguous splenic sections, it is apparent that the ratio of sense to antisense RNA is variable in immune cells of the spleen (Fig. 9E and F).

The importance of splenic ISH positivity is potentially exemplified in data obtained from an additional animal experiment, wherein we evaluated the concentration of infectious virus (PFU per milligram) in the spleen, liver, heart, and serum in A/J and C57BL/6J mice 3 days p.i. (n = 5/group) (Fig. 10A). There was no significant difference in the load of virus in the spleen or liver as determined by plaque assay; however, there was significantly more infectious virus present in the hearts ($P = 0.031$) and sera ($P = 0.026$) of A/J mice than there was in C57BL/6J mice. Most important and pertinent to disease pathogenesis was the level of ISH positivity for CVB3 genomic sequences in the spleen, liver, and heart tissues of A/J and C57BL/6J mice 3 days p.i. (Fig. 10B). There was a significant increase in the overall ISH positivity for CVB3 RNA in the spleens of C57BL/6J mice compared with that for A/J mice ($P = 0.0057$), which contrasts with significant decreases in positivity in the livers ($P = 0.047$) and hearts ($P = 0.026$) of A/J and C57BL/6J mice. Although liver ISH staining in C57BL/6J mice was significantly less than that in A/J mice at euthanasia (data not shown), when C57BL/6J mice die early after infection the intensity of ISH staining was increased (data not shown), suggesting fulminant virus infection as one possible cause of death. The infectious viral load in the hearts of A/J mice was significantly higher than that in C57BL/6J mice at days 4 and 5 p.i. (Fig. 11), suggesting that the latter mice are more effective at clearing the virus infection, albeit by an undetermined mechanism.

In vivo distribution of CVB3 antigens relative to splenic immune cells. Flow cytometry corroborates ISH in that viral antigen association with splenic immune cell subsets was observed in splenocytes from in vivo-infected A/J mice. Thus, composite flow cytometry analysis demonstrates that CVB3 antigen (R-phycoerythrin staining) is associated with 12% of the total splenocytes and 20 to 25% of the splenic lymphocytes after in vivo infection (Fig. 12). Of the splenic lymphocytes positive for viral antigen, 69.6% are B cells (fluorescein iso-

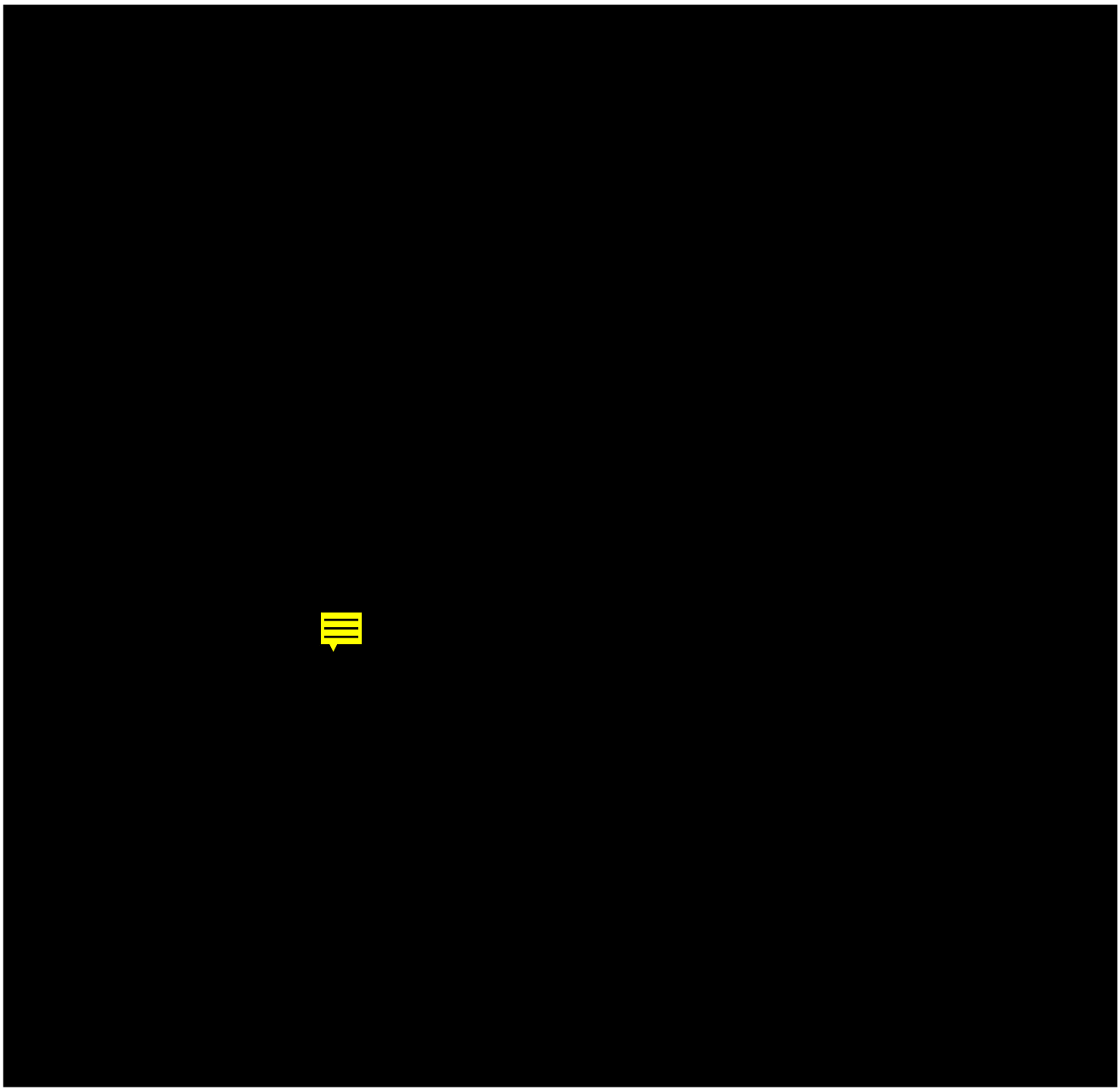

FIG. 9. ISH for sense-strand (A, C, and E) and antisense-strand (B, D, and F) RNA in spleens from A/J mice. Tissue sections were fixed at the time of euthanasia (A and B) or after 18 h of culture in nutrient media (C to F). Note the increase in ISH positivity in cultured tissues of both strains (C57BL/6J tissues are not shown) and the distinct hybridization for antisense-strand RNA in the A/J strain (F [arrowheads]). Positivity for antisense-strand RNA in cultured C57BL/6J splenic tissue is also present (data not shown). (D) Bar = 100 μm (also for panels A to C); (F) bar = 50 μm (also for panel E).

thiocyanate staining), and of the total splenocytes positive for viral antigen, 50.4% are B cells. Finally, in these series of experiments, B cells constitute approximately 47.1 and 44.1% of splenic lymphocytes and total splenocytes, respectively.

Contiguous splenic sections were used for ISH and stained by an IHC method for B cells (Fig. 13). These results demonstrate that the majority of viral RNA in the spleen was associated with a select population of B cells, specifically, germinal-center B cells (Fig. 13). By histological examination, however, a portion of follicular dendritic (53) cells of a germinal center are also positive for CVB3 RNA (Fig. 14).

DISCUSSION

These data demonstrate that CVB3 associates with and replicates in mixed murine splenocytes in vitro and in murine B cells and extrafollicular cells in vivo. The manner of CVB3 association within different compartments of the immune system corresponded to differential susceptibilities of C57BL/6J and A/J mice to CVB3-induced disease.

The presence of virus within immune organs probably represents a process of virus sequestration for subsequent immune system sensitization; however, the association of viruses with

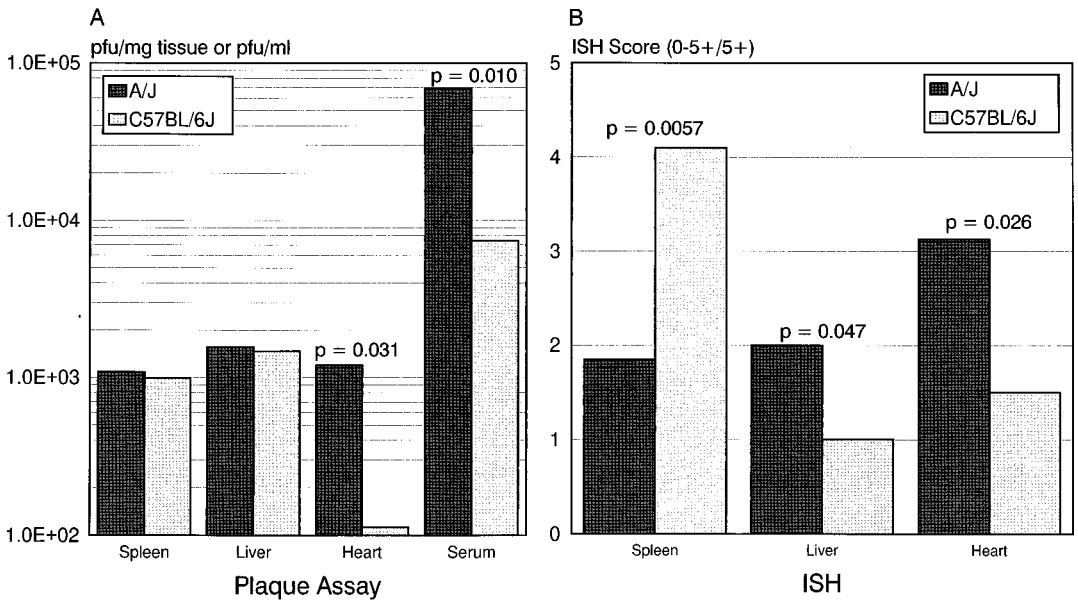

FIG. 10. Mean loads of infectious virus at day 3 p.i. in the spleens, livers, hearts, and sera of A/J and C57BL/6J mice ($n = 5$ per group). (A) There is significantly more infectious virus in the hearts ($P = 0.031$) and sera ($P = 0.010$) of A/J mice than in those of C57BL/6J mice as determined by plaque assay. (B) ISH staining for CVB3 is positive in the spleens, livers, and hearts of A/J and C57BL/6J mice ($n = 5$ per group). There is more overall mean ISH positivity (follicular and extrafollicular) in the spleens of infected C57BL/6J mice ($P = 0.0057$). This greater splenic ISH positivity in C57BL/6J mice is in contrast to the significantly lesser positivity in the livers ($P = 0.047$) and hearts ($P = 0.026$) of the same mice.

virtually every tissue and cellular element of the immune system (49) suggests that the nature of virus interactions with immune organs and immune cells in vivo will determine the consequences of such events.

The association or replication of enteroviruses in immune cells and/or immune cell lines has been demonstrated in vitro by a number of investigators. Thirty years ago poliovirus was suggested by electron microscopy to be present in leukocytes (48). Concurrently, other investigators (20) showed that multiplication of poliovirus occurred in leukocyte cultures. Human T- and B-lymphoid cell lines are permissive in vitro for replication of CVB serotypes by a carrier culture mechanism involving a minority of cells at any given time point (37, 61). Vuorinen et al. (61) have also reported that CVB3 replicates in T- and B-cell lines and in peripheral blood lymphocytes (PBL) after in vitro infection, although replication in PBL occurs at barely discernible levels. Others have contradictory data and have reported that CVB3 does not replicate in PBL infected in vitro (15). With regard to virus association with immune cells, Henke et al. (22) demonstrated that after incubation of pe-

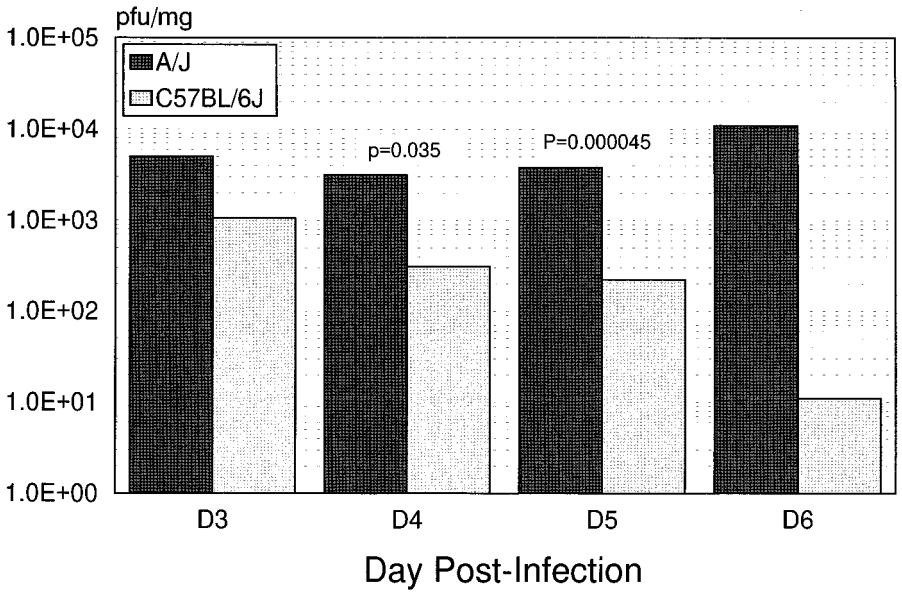

FIG. 11. Shown are the mean loads of virus (PFU per milligram) in heart tissues of C57BL/6J mice at days 3 to 6 p.i. versus those of A/J mice ($n = 7$ to 10 per group). Significantly less infectious virus is present in the myocardia of C57BL/6J animals at days 4 ($P = 0.035$) and 5 ($P = 0.000045$).

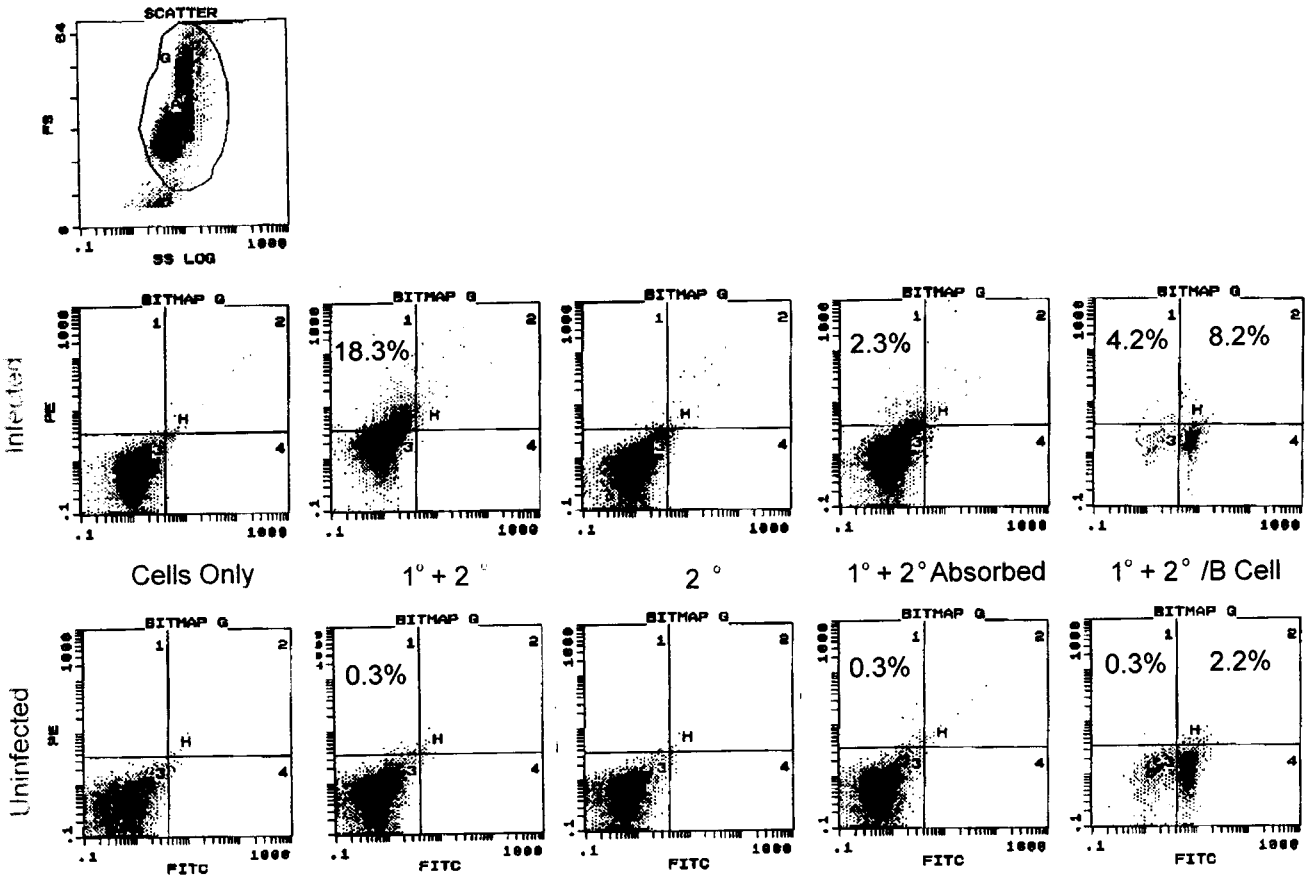

FIG. 12. Flow cytometric analysis for CVB3 antigen was performed on a sample of total splenocytes isolated from an in vivo-infected A/J mouse at day 3 p.i. (gate G of scatter plot). Results from this particular experiment of CVB3-infected and uninfected animals demonstrate that 16.0% (18.3% −2.3%) of total splenocytes are positive for CVB3, of which 6.0% (8.2% −2.2%) are B cells (shown by fluorescein isothiocyanate [FITC] staining) positive for CVB3 antigen (shown by R-phycoerythrin staining). Analysis of splenic lymphocytes (gate A of scatter plot [data not shown]) demonstrates that 20.5% of lymphocytes are positive for CVB3, of which 15.7% are B cells (shown by fluorescein isothiocyanate staining) positive for CVB3 antigen (shown by phycoerythrin staining). To ensure antigen specificity in recognition of activated and/or infected splenocytes, the following cells from CVB3-infected or uninfected animals were analyzed: unstained splenocytes (cells only) or splenocytes stained with the primary and secondary antibodies (1° + 2°), with the secondary antibody only (2°), or the primary and secondary antibodies, where the primary antibody was preabsorbed with 3,200 PFU of stock virus (1° + 2° Absorbed). The percent positive cells was determined from the difference between the percentages for 1° + 2° and 1° + 2° absorbed or 1° + 2°/B-cell percentages. Absence of positivity was evident when only the secondary antibody was used.

ripheral human mononuclear cells with CVB3 at a multiplicity of infection of 5 for 8 to 12 h, 19.2 to 33.2% of virus-exposed monocytes were positive for viral antigen by immunofluorescence. In a CVB3 murine model of myocarditis, we found that CVB3 is associated with splenocytes as determined by immunofluorescence (data not presented). Specifically, 12.9 to 17.4% of CD-8-positive T cells and 11 to 26% of adherent splenocytes were positive for viral antigen after in vitro infection and incubation (multiplicity of infection = 5, 12 h at 37°C). In the same experiments, the apparent permissiveness of purified B cells was even greater, resulting in prominent cytolysis.

CVB3-murine immune cell interactions. The present studies clearly demonstrate that myocarditic CVB3 does replicate in naive murine splenic lymphocytes early after in vitro infection (2, 4, 6, 8, 12, 24, and 48 h p.i.) (Fig. 1 to 3). Previous studies have looked at this issue but failed to demonstrate a productive CVB3 infection in splenocytes and peritoneal macrophages, and this was probably only because infectious particles were assayed at daily intervals p.i. (6, 38). Similarly, in vitro studies of CVB3 replication in murine lymphocytes and lymph node macrophages, performed by Gauntt et al. (18), revealed that "little or no replication of [CVB3] occurred in lymphocytes." It is clear from these and our own observations that daily evaluation of in vitro assay systems for infectious virus cannot reveal increases in virus titers in mixed splenocyte cultures, since the resulting data reflect bound uneclipsed virus, nascent virus, and virus inactivation (18). Overall, the amount of virus produced (nascent virus) is low.

Studies utilizing poliovirus have demonstrated that freshly isolated human leukocytes were unable to detectably support other than blastogenic replication through stimulation with phytohemagglutinin (63). Our model of mixed splenocyte cultures differs in that minimal production of infectious viral particles from nonstimulated and ConA-stimulated cells was detected; however, LPS-stimulated cells did not support virus production (Fig. 1C). It is interesting that the stimulation of infected cells with LPS did not result in the production of progeny virus detectable by plaque assay, although viral sense- and antisense-strand RNA were detectable by ISH and nested RT-PCR (Fig. 2 and 3). It is possible that LPS-activated macrophages, monocytes, and B cells and LPS-induced proinflammatory antiviral mediators such as interferons and nitric oxide (29) allowed efficient inactivation of CVB3 and thus limited the apparent production and detection of progeny infectious virus. Furthermore, the variability of virus titers detected in

FIG. 13. ISH (A and C) and IHC (B and D) demonstrate colocalization of CVB3 sense-strand RNA with a subset of B220-positive B cells (A and B [A/J]; C and D [C57BL/6J]) in the spleens of CVB3-infected animals at day 3 p.i. Colocalization is restricted primarily to germinal-center B cells. (B) Bar = 50 μm.

vitro in our murine models (Fig. 1) is likely a reflection of the different levels of permissiveness of splenocytes as derived from different murine donors. Studies of poliovirus infections in vitro support this notion of donor-dependent variability in permissiveness, since poliovirus replication can range from 1 to 14 PFU/day per infected human PBL (55). The subtlety and rapidity of eclipse and in vitro CVB3 replication we have observed in mixed splenocytes is concordant with the data on poliovirus infection of immune cells.

Studies of Gomez et al. (19) demonstrated that particular adherent cells, T cells, and B cells from the peripheral blood and spleens of CVB3-infected mice are associated with infectious virus as determined by plaque assays at 2, 3, and 4 days p.i. However, the nature of these associations has been questioned and remains unanswered (6). Our data characterizing the in vivo temporal load of virus in the spleens of infected animals (Fig. 4) corroborate previously published data on the viral titers in spleens of CVB3-infected CD-1 mice (18). Furthermore, the in vivo association and replication of CVB3 in particular immune cells are one likely source of infected peripheral blood cells as previously demonstrated by Gomez et al. (19). Of potential importance, the localization of virus by IHC, especially in the spleen, appears much less sensitive than the hybridization methodology for detecting viral RNA that is presented in this study.

The presence of sense- and antisense-strand RNA, indicating replication of CVB3 RNA in the spleens of infected A/J and C57BL/6J mice, was documented by nested RT-PCR (Fig. 3). This replication is further corroborated by ISH positivity for antisense-strand RNA in splenic germinal centers of CVB3-infected A/J mice at autopsy (Fig. 8) and in cultured explant splenic sections (Fig. 9) from both A/J and C57BL/6J CVB3-infected mice. The primary cellular constituent of a germinal center is the B cell (34, 58), which is the cell phenotype with which CVB3 associates in vivo (Fig. 13). As noted above, we have detected sense-strand RNA in the lymph nodes of infected animals; however, as with the spleen cells in the present studies, a more complete and systematic evaluation of lymph nodes to determine the presence of the antisense-strand RNA is warranted. With regard to the level of replication in splenic immune cells of A/J and C57BL/6J mice, these in vitro and in vivo data indicate that CVB3 replicates (RNA and infectious particles) more efficiently in the A/J than in the C57BL/6J murine strain. Plaque assay data presented by Huber et al. (26) indicated that CVB3 variants replicate in a BALB/c monocyte cell line; however, the more virulent, myocarditic variant of CVB3 replicated to titers higher than those of the less virulent, nonmyocarditic variant. Thus, the regulation of CVB3 replication may be critical in the interaction of CVB3 and a host. Kandolf and colleagues (23, 31) have established that the ratio of sense to antisense strands of viral RNA is 100:1 during early infection of the myocardium and is 1:1 during persistent infection. These data suggest that one possible mechanism of establishing a persistent infection is the differential regulation of viral RNA strand synthesis. Furthermore, the regulation of viral RNA synthesis has been implicated in the virulence of CVB3 (60). In our model (Fig. 9E and F), the varying ratios of sense to antisense viral RNA strands in the spleens of A/J mice

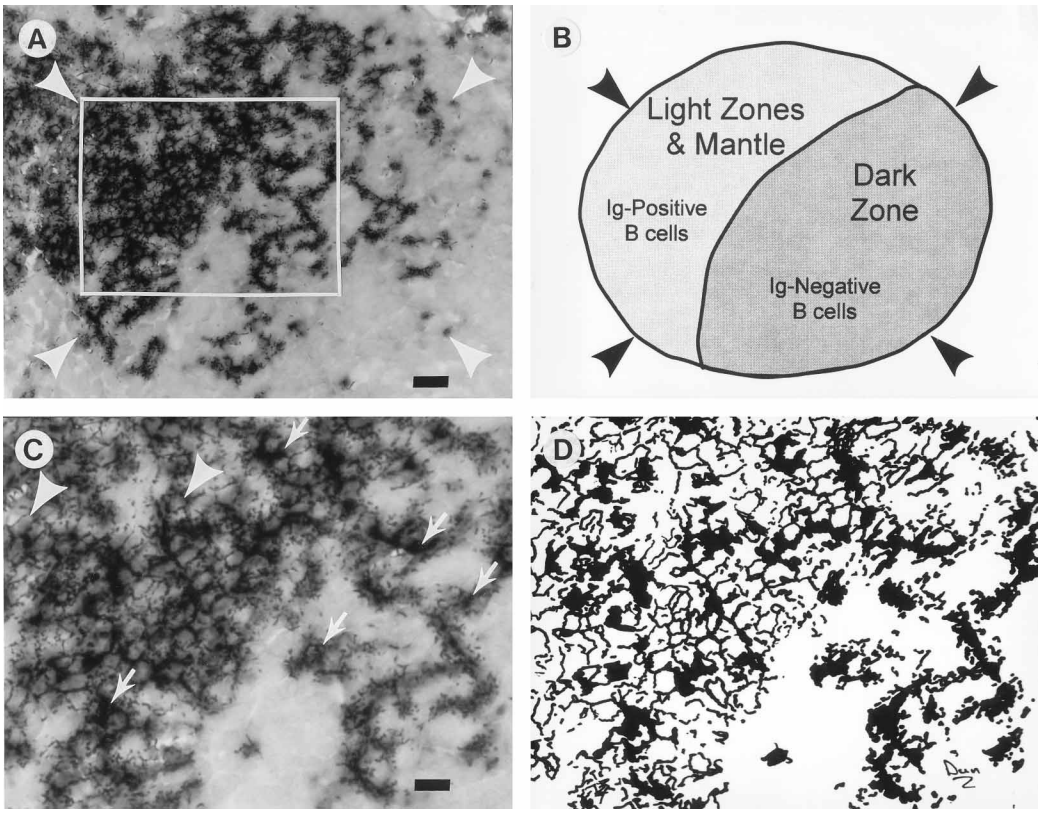

FIG. 14. ISH staining for CVB3 in the spleen of a C57BL/6J mouse at day 3 p.i. is shown (A), and an enlargement of the boxed region is illustrated (C). A schematic of zones of the germinal center (B), delineated by arrowheads in panels A and B, depicts the immunoglobulin-negative (dark zone) and immunoglobulin-positive (mantle and light zones) regions. (D) A tracing of the ISH signal (C) depicts the characteristic pattern of viral RNA-antigen retention. Follicular dendritic cells and B cells in the germinal center are indicated by arrows and arrowheads, respectively. (A) Bar = 20 μm; (C) bar = 10 μm.

may indicate a developing persistent CVB3 infection within particular immune cells. This phenomenon has been previously described for lymphocytic choriomeningitis virus infections (30, 36) and suggests that the high level of systemic replication of CVB3 in A/J mice may lead to the production of mutant progeny which are able to replicate more efficiently in immune cells. Evidence obtained by ISH and nested RT-PCR has provided a measure of actual virus replication in the spleens of CVB3-infected animals. The distribution and intensity of hybridization for the sense strand more readily reflected and correlated to the relative load (PFU per milligram) of infectious virus (Fig. 6 and 7). Further, these correlations likely reflect the systemic viral load, which seeds the spleen with infectious CVB3 and stimulates a correlative immune response, resulting in concordant trapping of infectious virus. The question remains: does extrafollicular localization of CVB3 affect susceptibility to myocarditis (Fig. 5)?

CVB3 clearly replicates in murine spleens early after in vivo infection (1 to 7 days p.i.), and the localization of infectious, replicating virus to germinal centers and extrafollicular cells most likely reflects two events of a CVB3 infection: an adaptive antiviral immune response by the host and a disadvantageous association of virus and immune cells. The classical immunological event in the spleen during CVB3 infection is the adaptive immune response with immune sensitization and generation of polyclonal germinal centers (35, 58). A second and adverse event of CVB3 infection is the association of replicating CVB3 with select B cells, follicular dendritic cells (FDC), and extrafollicular cells. It is reasonable to hypothesize that virus replication perturbs the normal function of immune cells and thus disrupts the homeostasis of an immunological response to antigens. This hypothesis stems from our demonstration by ISH and flow cytometry of viral RNA and antigen positivity localized to immune cells (Fig. 3, 6, 8, 9, and 12). As well, other investigators have demonstrated that in vitro functional assays of lymphoid cells are suppressed after infection with CVB3 and that this function is restored by supplementation with peritoneal macrophages (38). Evidence of CVB3-induced splenic involution due to dysfunctional macrophages further supports the theory that CVB3 perturbs immune function (38). We and others have shown that the in vivo immune response to a third-party antigen (sheep erythrocytes) is decreased after CVB3 infection and is likely due to the impairment of antigen presentation (4, 7); however, the level of macrophage saturation by phagocytosed material, and thus potential antigenic competition for histocompatibility antigens, must be kept in mind when evaluating these data (5).

The CVB3 model of infection with its dramatic splenic involution is in contrast to other viral infections such as lymphocytic choriomeningitis virus-induced splenic hypertrophy (3, 51) and is thought to reflect immune cell proliferation and the retention of antigen-specific lymphocytes in the early stages of infection. It should be noted, however, that with lymphocytic choriomeningitis virus-induced splenomegaly there are dysregulation and suppression of immune responses which result in histological disturbances and impaired antigen presentation (3, 66). This impairment is hypothetically related to the association of viral antigen with marginal-zone and red-pulp mac-

rophages and the destruction of these cells by cytotoxic antiviral immune responses (3, 36). Thus, massive involution of the spleen after CVB3 infection probably results from severe perturbations of the normal immune response through the replication of CVB3 in B cells (Fig. 8, 9, and 13) and/or macrophages.

The interaction of CVB3 with the immune cells in the spleen of infected mice is undoubtedly a complex one. As depicted in Fig. 14A to D, ISH staining for CVB3 RNA reflects the characteristic pattern of a germinal center (35, 58) with antigen retention and stimulation of the immune response in a secondary lymphoid organ. Virus-immune complexes first localize to FDCs within the FDC network. The ISH positivity data for viral RNA are reminiscent of the tentacular shape and distribution of such FDCs (Fig. 14C, arrows). ISH positivity for viral RNA in the cuff of the germinal center (Fig. 14C, arrowheads) is characteristic of B cells undergoing antigen-specific selection, hypermutation, and maturation (35, 58). This ISH-positive staining for viral RNA in the outer zones of a germinal center (the basal light zone, the apical light zone, and the follicular mantle) is reminiscent of centriocytes which are immunoglobulin positive and which trap virus antigen, as reflected by the halo staining of germinal center cells (Fig. 14C, arrowheads). Thus, the bulk of ISH positivity in the spleen is largely a reflection of the adaptive immune response to CVB3 infection and retention of viral antigen, viral particles, and thus viral RNA. The disturbances of antigen presentation described are, however, potentially due to the replication of CVB3 in a minority of splenocytes and specifically in B cells or extrafollicular cells.

Our data provide a window of insight into the distinctly different myocardial susceptibilities of A/J and C57BL/6J mice to CVB3 (Fig. 11) (12). Indeed, given that CVB3 associates with and replicates in murine splenic immune cells in vitro and in vivo, the precise nature of CVB3 association with B cells, FDC, marginal-zone macrophages, red-pulp macrophages, PBL, and Kupffer cells requires closer analysis. The consequence of such interactions on the progression of CVB3-induced diseases is potentially profound. These events may be paramount to end-organ susceptibility and the development of virus-induced disease in different strains of mice and in humans.

ACKNOWLEDGMENTS

We deeply appreciate the technical support of Lubos Bohunek. As well, we recognize the support and consultation of Lawrence Haley, regarding flow cytometric analysis, and the fine editorial and photographic contributions of Shelley Wood and Stuart Green.

These studies have been supported by the American Heart Association, the British Columbia Health Research Foundation, and the Heart and Stroke Foundation of British Columbia and Yukon (B.M.M.) and by the M.D./Ph.D. program of the Department of Pathology and Microbiology, University of Nebraska Medical Center, Omaha, Nebr. (D.R.A.).

REFERENCES

1. **Ahmed, R., C.-C. King, and M. B. A. Oldstone.** 1987. Virus-lymphocyte interaction: T cells of the helper subset are infected with lymphocytic choriomeningitis virus during persistent infection in vivo. J. Virol. **61:** 1571–1576.
2. **Ahmed, R., and M. B. A. Oldstone.** 1988. Organ specific selection of viral variants during chronic infection. J. Exp. Med. **167:**1719–1724.
3. **Althage, A., B. Odermatt, D. Moskophidis, T. Kundig, U. Hoffman-Rohrer, H. Hengartner, and R. M. Zinkernagel.** 1992. Immunosuppression by lymphocytic choriomeningitis virus infection: competent effector T and B cells but impaired antigen presentation. Eur. J. Immunol. **22:**1803–1812.
4. **Anderson, D. R., J. E. Wilson, G. J. Dougherty, and B. M. McManus.** Unpublished data.

4a. **Anderson, K. S., J. E. Wilson, D. R. Anderson, D. C. Yang, K. Klingel, and B. M. McManus.** Submitted for publication.

5. **Babbitt, B. P., G. Matsueda, E. Haber, E. R. Unanue, and P. M. Allen.** 1986. Antigenic competition at the level of peptide-Ia binding. Proc. Natl. Acad. Sci. USA **83:**4509–4513.
6. **Bendinelli, M., P. C. Conaldi, and D. Matteucci.** 1988. Interactions with the immune system, p. 81–102. *In* M. Bendinelli and H. Friedman (ed.), Coxsackieviruses: a general update. Plenum Press, New York.
7. **Bendinelli, M., D. Matteucci, A. Toniolo, A. M. Patane, and M. P. Pistillo.** 1982. Impairment of immunocompetent mouse spleen cell functions by infection with coxsackievirus B3. J. Infect. Dis. **146:**797–805.
8. **Bergelson, J. M., J. G. Mohanty, R. L. Crowell, N. F. St. John, D. M. Lublin, and R. W. Finberg.** 1995. Coxsackievirus B3 adapted to growth in RD cells binds to decay-accelerating factor (CD55). J. Virol. **69:**1903–1906.
9. **Blay, R., K. Simpson, K. Leslie, and S. Huber.** 1989. Coxsackievirus-induced disease: CD4+ cells initiate both myocarditis and pancreatitis in DBA/2 mice. Am. J. Pathol. **135:**899–907.
10. **Chapman, N. M., S. Tracy, C. J. Gauntt, and U. Fortmueller.** 1990. Molecular detection and identification of enteroviruses using enzymatic amplification and nucleic acid hybridization. J. Clin. Microbiol. **28:**843–850.
11. **Chow, L. H., K. W. Beisel, and B. M. McManus.** 1992. Enteroviral infection of mice with severe combined immunodeficiency. Evidence for direct viral pathogenesis of myocardial injury. Lab. Invest. **66:**24–31.
12. **Chow, L. H., C. J. Gauntt, and B. M. McManus.** 1991. Differential effects of myocarditic variants of coxsackievirus B3 in inbred mice: a pathologic characterization of heart tissue damage. Lab. Invest. **64:**55–64.
13. **Coligan, J. E., A. M. Kruisbeek, D. H. Margulies, E. M. Shevach, and W. Strober.** 1994. *In vitro* assays for mouse lymphocyte function, p. 3.1.2–3.1.5. *In* R. Coico (ed.), Current protocols in immunology, vol. 1. John Wiley and Sons, Inc., New York.
14. **Coligan, J. E., A. M. Kruisbeek, D. H. Margulies, E. M. Shevach, and W. Strober.** 1994. Measurements of proliferative responses of cultured lymphocytes, p. 7.10.1–7.10.6. *In* R. Coico (ed.), Current protocols in immunology, vol. 2. John Wiley and Sons, Inc., New York.
15. **Dagan, R., and M. A. Menegus.** 1992. Replication of enteroviruses in human mononuclear cells. Isr. J. Med. Sci. **28:**369–372.
16. **Embretson, J., M. Zupancic, J. L. Ribas, A. Burke, P. Racz, K. Tenner-Racz, and A. T. Haase.** 1993. Massive covert infection of helper T lymphocytes and macrophages by HIV during the incubation period of AIDS. Nature (London) **362:**359–362.
17. **Gauntt, C. J., H. M. Arizpe, A. L. Higdon, H. J. Wood, D. F. Bowers, M. M. Rozek, and R. Crawley.** 1995. Molecular mimicry, anti-coxsackievirus B3 neutralizing monoclonal antibodies, and myocarditis. J. Immunol. **154:**2983–2995.
18. **Gauntt, C. J., M. D. Trousdale, D. R. LaBadie, R. E. Paque, and T. Nealon.** 1979. Properties of coxsackievirus B3 variants which are amyocarditic or myocarditic for mice. J. Med. Virol. **3:**207–220.
19. **Gomez, M. P., M. P. Reyes, F. Smith, L. K. Ho, and A. M. Lerner.** 1980. Coxsackievirus B3-positive mononuclear leukocytes in peripheral blood of Swiss and athymic mice during infection (40942). Proc. Soc. Exp. Biol. Med. **165:**107–113.
20. **Gresser, I., and C. Chany.** 1964. Multiplication of poliovirus type I in preparations of human leukocytes and its inhibition by interferon. J. Immunol. **92:**889–895.
21. **Hay, R. J.** 1986. Preservation and characterization, p. 86–89. *In* R. I. Freshney (ed.), Animal cell culture: a practical approach. IRL Press Limited, Washington, D.C.
22. **Henke, A., C. Mohr, H. Sprenger, C. Graebner, A. Stelzner, M. Nain, and D. Gemsa.** 1992. Coxsackievirus B3-induced production of tumor necrosis factor-alpha, IL-1 beta, and IL-6 in human monocytes. J. Immunol. **148:**2270–2277.
23. **Hohenadl, C., K. Klingel, J. Mertsching, P. H. Hofschneider, and R. Kandolf.** 1991. Strand-specific detection of enteroviral RNA in myocardial tissue by in situ hybridization. Mol. Cell. Probes. **5:**11–20.
24. **Holland, B. S., and M. D. Copenhauer.** 1987. An improved sequentially rejective Bonferroni test procedure. Biometrics **43:**417–423.
25. **Huber, S. A., D. C. Lyden, and P. A. Lodge.** 1985. Immunopathogenesis of experimental coxsackievirus induced myocarditis: role of autoimmunity. Herz **10:**1–7.
26. **Huber, S. A., J. Polgar, P. Schultheiss, and P. Schwimmbeck.** 1994. Augmentation of pathogenesis of coxsackievirus B3 infections in mice by exogenous administration of interleukin-1 and interleukin-2. J. Virol. **68:**195–206.
27. **Innis, M. A., and D. H. Gelfand.** 1990. Optimization of PCRs, p. 3–12. *In* M. A. Innis, D. H. Gelfand, J. J. Sninsky, and T. J. White (ed.), PCR protocols: a guide to methods and applications. Academic Press, Inc., San Diego, Calif.
28. **Jin, O., M. J. Sole, J. W. Butany, W. K. Chia, P. R. McLaughlin, P. Liu, and C. C. Liew.** 1990. Detection of enterovirus RNA in myocardial biopsies from patients with myocarditis and cardiomyopathy using gene amplification by polymerase chain reaction. Circulation **82:**8–16.
29. **Karupiah, G., Q. W. Xie, R. M. Buller, C. Nathan, C. Duarte, and J. D. MacMicking.** 1993. Inhibition of viral replication by interferon-gamma-induced nitric oxide synthase. Science **261:**1445–1448.
30. **King, C.-C., R. de Fries, S. R. Kolhekar, and R. Ahmed.** 1990. In vivo

selection of lymphocyte-tropic and macrophage-tropic variants of lymphocytic choriomeningitis virus during persistent infection. J. Virol. **64:**5611–5616.
31. **Klingel, K., C. Hohenadl, A. Canu, M. Albrecht, M. Seemann, G. Mall, and R. Kandolf.** 1992. Ongoing enterovirus-induced myocarditis is associated with persistent heart muscle infection: quantitative analysis of virus replication, tissue damage, and inflammation. Proc. Natl. Acad. Sci. USA **89:**314–318.
32. **Klump, W. M., I. Bergmann, B. C. Müller, D. Ameis, and R. Kandolf.** 1990. Complete nucleotide sequence of infectious coxsackievirus B3 cDNA: two initial 5′ uridine residues are regained during plus-strand RNA synthesis. J. Virol. **64:**1573–1583.
33. **Krajewski, S., S. Bodrug, R. Gascoyne, K. Berean, M. Krajewska, and J. C. Reed.** 1994. Immunohistochemical analysis of *mcl-1* and *bcl-2* proteins in normal and neoplastic lymph nodes. Am. J. Pathol. **145:**515–525.
34. **Kroese, F. G. M., H. G. Seijen, and P. Nieuwenhuis.** 1987. Germinal centers develop oligoclonally. Eur. J. Immunol. **17:**1069–1072.
35. **Liu, Y.-J., G. D. Johnson, J. Gordon, and I. C. M. MacLennan.** 1992. Germinal centres in T-cell-dependent antibody responses. Immunol. Today **13:**17–21.
36. **Matloubian, M., S. R. Kolhekar, T. Somasundaram, and R. Ahmed.** 1993. Molecular determinants of macrophage tropism and viral persistence: importance of single amino acid changes in the polymerase and glycoprotein of lymphocytic choriomeningitis virus. J. Virol. **67:**7340–7349.
37. **Matteucci, D., M. Paglianti, A. M. Giangregorio, M. R. Capobianchi, F. Dianzani, and M. Bendinelli.** 1985. Group B coxsackieviruses readily establish persistent infections in human lymphoid cell lines. J. Virol. **56:**651–654.
38. **Matteucci, D., A. Toniolo, P. G. Conaldi, F. Basolo, Z. Gori, and M. Bendinelli.** 1985. Systemic lymphoid atrophy in coxsackievirus B3-infected mice: effects of virus and immunopotentiating agents. J. Infect. Dis. **151:**1100–1108.
39. **McChesney, M. B., and M. B. A. Oldstone.** 1987. Viruses perturb lymphocyte functions: selected principles characterizing virus-induced immunosuppression. Annu. Rev. Immunol. **5:**279–304.
40. **McManus, B. M., D. R. Anderson, G. A. Perry, J. E. Wilson, and R. Kandolf.** 1992. Immunocyte interaction with coxsackievirus B3m in murine models of enteroviral myocarditis: possible role of the spleen and lymph nodes as viral reservoirs. Circulation **86:**I–57.
41. **McManus, B. M., L. H. Chow, J. E. Wilson, D. R. Anderson, J. M. Gulizia, C. J. Gauntt, K. E. Klingel, K. W. Beisel, and R. Kandolf.** 1993. Direct myocardial injury by enterovirus: a central role in the evolution of murine myocarditis. Clin. Immunol. Immunopathol. **68:**159–169.
42. **McManus, B., L. H. Chow, J. E. Wilson, D. R. Anderson, and R. Kandolf.** 1993. Direct damage of myocardium by enterovirus, p. 284–293. *In* H. R. Figulla, R. Kandolf, and B. McManus (ed.), Idiopathic dilated cardiomyopathy: cellular and molecular mechanisms, clinical consequences. Springer-Verlag, Berlin.
43. **McManus, B. M., and R. Kandolf.** 1991. Evolving concepts of cause, consequence, and control in myocarditis. Curr. Opin. Cardiol. **6:**418–427.
44. **McManus, J. E., D. C. Yang, R. Zehebr, D. R. Anderson, G. P. Bondy, and B. M. McManus.** 1995. In situ hybridization for viral RNA: a comparison of manual and automated methods. FASEB J. **9:**A970.
45. **Melnick, J. L.** 1956. Tissue culture methods for the cultivation of poliovirus and other viruses, p. 97–152. *In* T. Francis (ed.), Diagnostic procedures for viral and rickettsial diseases. American Public Health Association, New York.
46. **Meyers, T. W., and D. H. Gelfand.** 1991. Reverse transcription and DNA amplification by a *Thermus thermophilus* DNA polymerase. Biochemistry **30:**7661–7666.
47. **Mims, C. A.** 1964. Aspects of the pathogenesis of virus diseases. Bacteriol. Rev. **28:**30–71.
48. **Nelson, E., H. Hager, and E. Kovacs.** 1963. Virus-containing leukocytes in polioencephalitis. Science **139:**499–599.
49. **Notkins, A. L., S. E. Mergenhagen, and R. J. Howard.** 1970. Effect of virus infections on the function of the immune system. Annu. Rev. Microbiol. **24:**525–538.
50. **Pantaloe, G., C. Graziosi, J. F. Demarest, L. Butini, M. Montroni, C. H. Fox, J. M. Orenstein, D. P. Kotler, and A. S. Fauci.** 1993. HIV infection is active and progressive in lymphoid tissue during the clinically latent stage of disease. Nature (London) **362:**355–358.
51. **Razvi, E. S., Z. Jiang, B. A. Woda, and R. M. Welsh.** 1995. Lymphocyte apoptosis during the silencing of the immune response to acute viral infections in normal, Ipr, and Bcl-2-transgenic mice. Am. J. Pathol. **147:**79–91.
52. **Redenbach, K. S., D. R. Anderson, J. E. Wilson, and B. M. McManus.** 1995. Improved detection of enterovirus due to optimization and nesting of polymerase chain reaction. Presented at the Society for Cardiovascular Pathology Young Investigators Symposium, USCAP, 11 March 1995.
53. **Schriever, F., and L. M. Nadler.** 1992. The central role of follicular dendritic cells in lymphoid tissues. Adv. Immunol. **51:**243–284.
54. **Shafren, D. R., R. C. Bates, M. V. Agrez, R. L. Herd, G. F. Burns, and R. D. Barry.** 1995. Coxsackieviruses B1, B3, and B5 use decay accelerating factor as a receptor for cell attachment. J. Virol. **69:**3873–3877.
55. **Soontiens, F. J. C. J., and J. Van Der Veen.** 1973. Evidence for a macrophage-mediated effect of poliovirus on the lymphocyte response to phytohemagglutinin. J. Immunol. **111:**1411–1419.
56. **Stoddart, C. A., R. D. Cardin, J. M. Boname, W. C. Manning, G. B. Abenes, and E. S. Mocarski.** 1994. Peripheral blood mononuclear phagocytes mediate dissemination of murine cytomegalovirus. J. Virol. **68:**6243–6253.
57. **Systat, Inc.** 1992. Systat for windows: statistics, version 5, p. 750. Systat, Inc., Evanston, Ill.
58. **Thorbecke, G. J., A. R. Amin, and V. K. Tsiagbe.** 1994. Biology of germinal centers in lymphoid tissue. FASEB J. **8:**832–840.
59. **Tse, W. T., and B. G. Forget.** 1990. Reverse transcription and direct amplification of cellular RNA transcripts by *Taq* polymerase. Gene **88:**293–296.
60. **Tu, Z., N. M. Chapman, G. Hufnagel, S. Tracy, J. R. Romero, W. H. Barry, L. Zhao, K. Currey, and B. Shapiro.** 1995. The cardiovirulent phenotype of coxsackievirus B3 is determined at a single site in the genomic 5′ nontranslated region. J. Virol. **69:**4607–4618.
61. **Vuorinen, T., R. Vainionpaa, H. Kettinen, and T. Hyypia.** 1994. Coxsackievirus B3 infection in human leukocytes and lymphoid cell lines. Blood **84:**823–829.
62. **Wheelock, E. F., and S. T. Toy.** 1970. Participation of lymphocytes in viral infections. Adv. Immunol. **16:**123–184.
63. **Willems, F. T. C., J. L. Melnick, and W. E. Rawls.** 1969. Replication of poliovirus in phytohemagglutinin-stimulated human lymphocytes. J. Virol. **3:**451–457.
64. **Wolfgram, L. J., and N. R. Rose.** 1989. Coxsackievirus infection as a trigger of cardiac autoimmunity. Immunol. Res. **8:**61–80.
65. **Woodruff, J. F.** 1980. Viral myocarditis. A review. Am. J. Pathol. **101:**425–484.
66. **Wu-Hsieh, B., D. H. Howard, and R. Ahmed.** 1988. Virus-induced immunosuppression: a murine model of susceptibility to opportunistic infection. J. Infect. Dis. **158:**232–235.

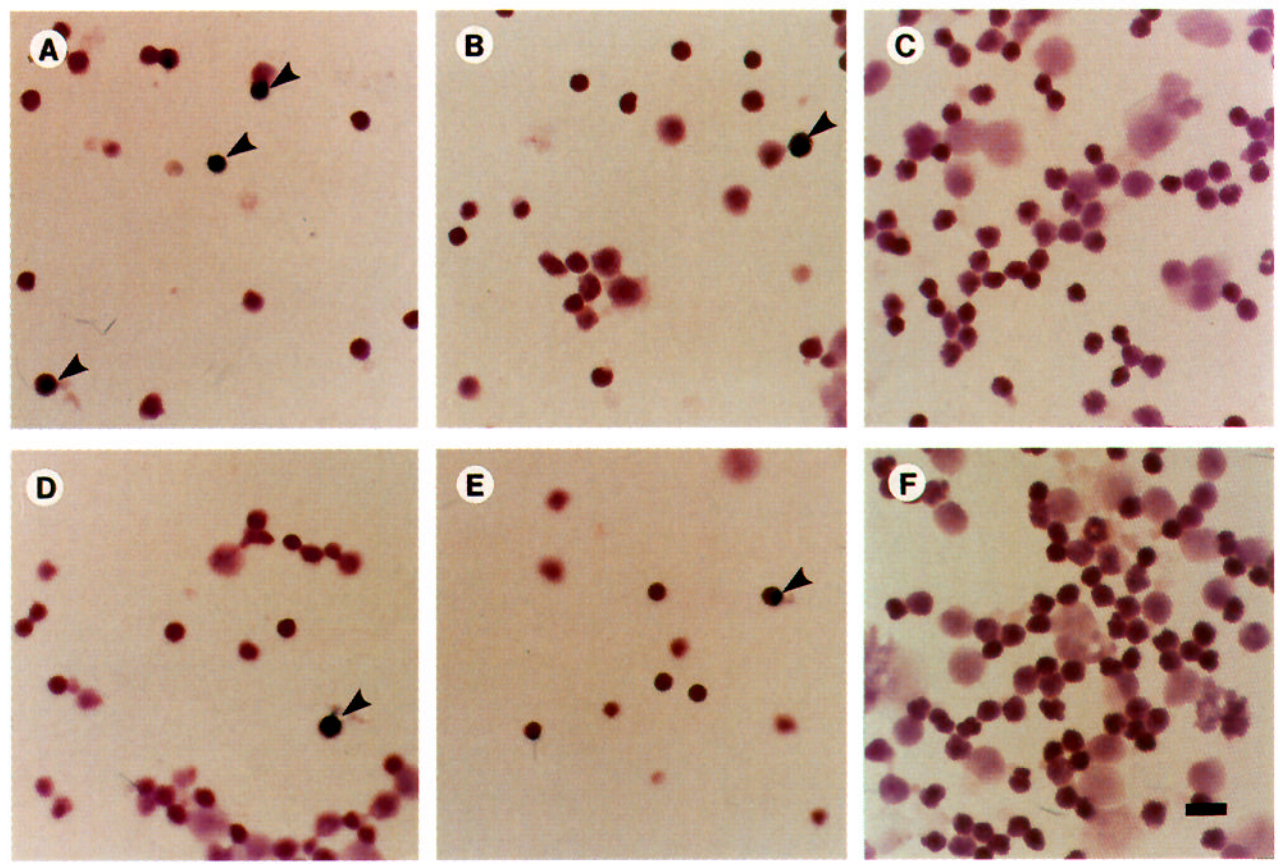
A
B
C
D
E
F

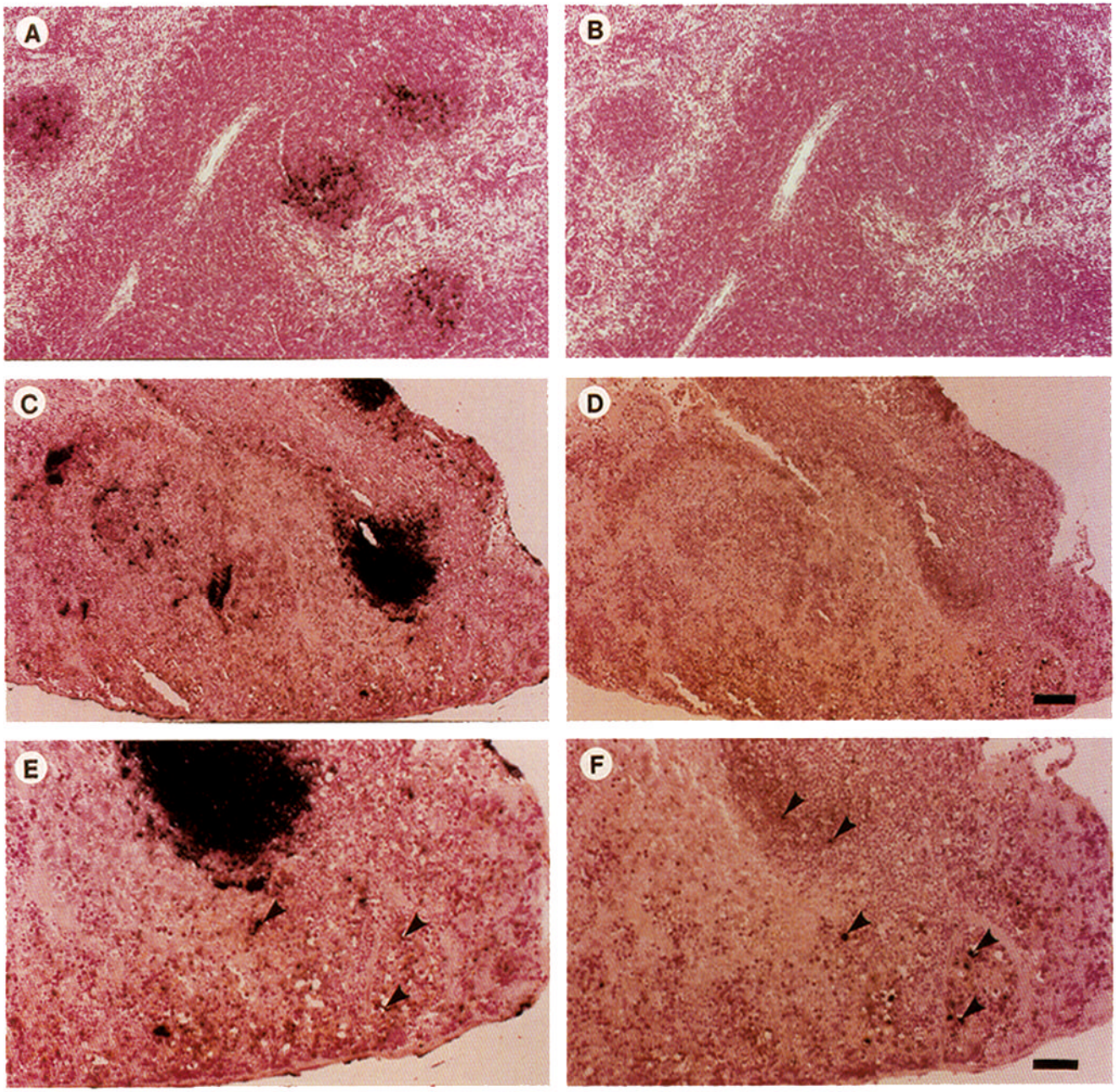
A
B
C
D
E
F

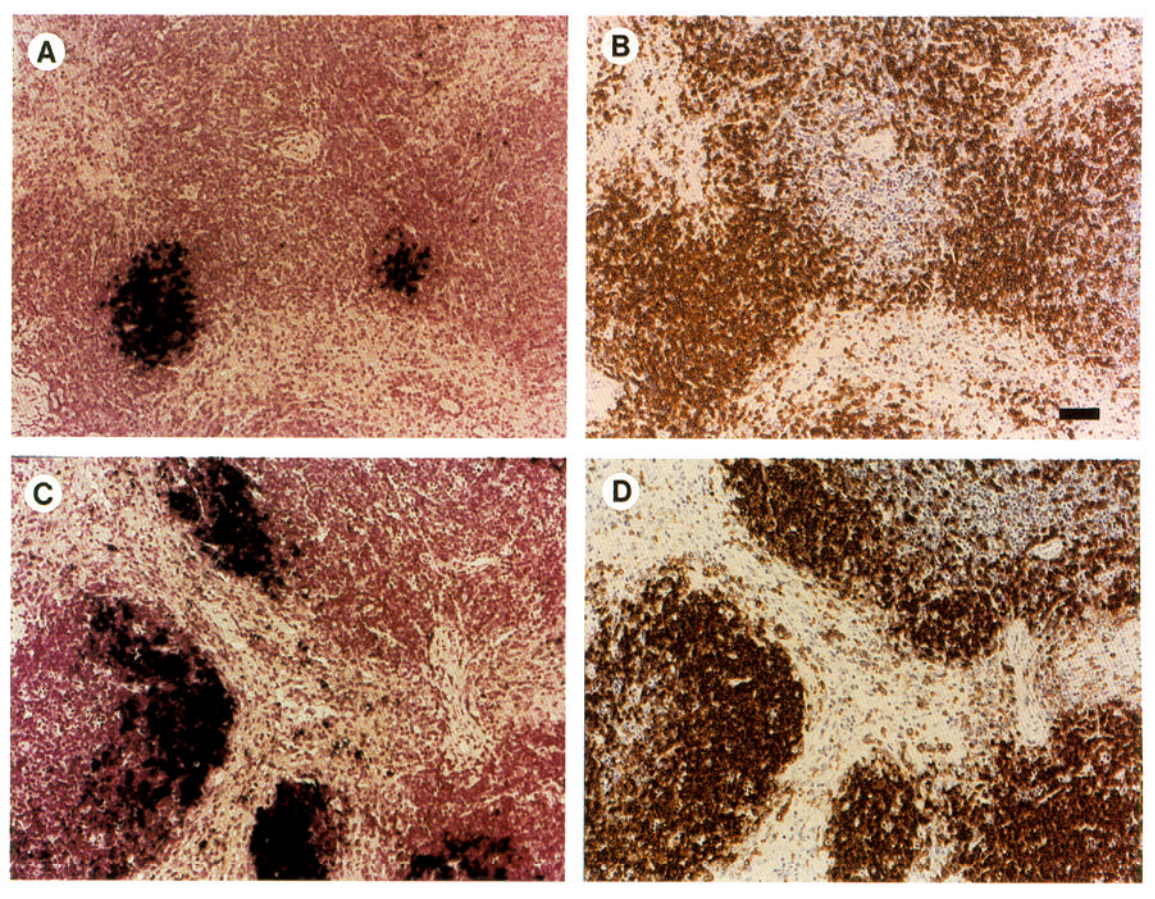
A
B
C
D